Methanol synthesis from CO_2 using a silicone rubber/ceramic composite membrane reactor

Guangwen Chen, Quan Yuan*

Dalian Institute of Chemical Physics, Chinese Academy of Sciences, 457 Zhongshan Road, Dalian 116023, PR China

Abstract

A one-dimensional isothermal pseudo-homogeneous parallel flow model was developed for the methanol synthesis from CO_2 in a silicone rubber/ceramic composite membrane reactor. The fourth-order Runge–Kutta method was adopted to simulate the process behaviors in the membrane reactor. How those parameters affect the reaction behaviors in the membrane reactor, such as Damköhler number Da, pressure ratio p_r, reaction temperature T, membrane separation factor α, membrane permeation parameter Φ, as well as the non-uniform parameter of membrane permeation L_1, were discussed in detail. Parts of the theoretical results were tested and verified; the experimental results showed that the conversion of the main reaction in the membrane reactor increased by 22% against traditional fixed bed reactor, and the optimal non-uniform parameter of membrane permeation rate, $L_{1,opt}$, does exist.
© 2003 Elsevier B.V. All rights reserved.

Keywords: CO_2 hydrogenation; Damköhler number; Fixed bed reactor; Membrane separation factor; Non-uniform permeation

1. Introduction

A membrane reactor is a system or device which combines membranes and chemical reactions [1]. The applications of membrane reaction technology in chemical reaction processes now are mainly focused on the reaction systems containing hydrogen or oxygen that are based on inorganic membranes such as Pd membrane [2–5] and ceramic membrane [6,7]. In recent years, with the development of membrane materials, membrane reaction technology has been gaining a promising prospect in the field of the synthesis of oxy-organic compounds. Struis [8] studied

the synthesis of methanol from CO_2 using a Nafion® membrane because of its ability of preferential permeation of products such as methanol and water. The results indicated that membrane reactor has a higher conversion than traditional fixed bed reactor. However, the application is limited since the allowed working temperature of this membrane is lower than 200 °C.

The preparation of a defect-free composite membrane with high selectivity, high permeation rate and severe-condition resistance, is a key topic for further development of membrane science and technology. At present, the majority of the commercialized membranes are made from organic polymers due to their higher inherent selectivity and easier fabrication. However, these materials usually show limited stability under severe circumstances, such as high temperatures, high pressures and in organic solvents.

* Corresponding author. Tel.: +86-411-468-7994; fax: +86-411-469-1570.

E-mail address: qyuan@dicp.ac.cn (Q. Yuan).

Nomenclature

A_m	membrane area (m^2)
Da	Damköhler number, $\rho V k_{1,0}/F_0$
F	mole flux in reaction side (mol/s)
f	dimensionless reaction rate function
J	permeation rate ml/cm^2 s cmHg
K_i	adsorption equilibrium constant of component i, 10/MPa
K_p	chemical equilibrium constant
k_+	reaction rate constant (mol/g h)
L	total length of catalyst bed (m)
L_1	non-uniform membrane permeation rate parameter
l	axial position of reactor (m)
l_1	membrane length with permeation (m)
l_m	thickness of membrane (m)
N	membrane flux (mol/s)
P	membrane permeability, ml cm/s cm^2 cmHg
p	pressure, 0.1 Mpa
p_r	pressure ratio of both side of membrane, p_l/p_h
Q	mole flux of permeate side (mol/s)
q_1	flux ratio of purge gas to feed gas
R	universal gas constant (J/mol K)
r	reaction rate (mol/g h)
S	Radial section area of reactor (m^2)
T	temperature, °C (K)
V_{cat}	volume of catalyst (ml)
W	weight of catalyst (g)
X	reaction conversion
X_e	equilibrium conversion
x	mole component of reaction side
y	mole component of permeate side
z	dimensionless axial position of reactor

Greek letters

α	apparent separation factor of membrane
γ	mole ratio of feed
υ	stoichiometry coefficient
ρ	packed density of catalyst, g/ml
Φ	dimensionless parameter of membrane permeation rate

Subscripts

0	initial value or reactor inlet
1	main reaction
h	reaction side
i	component
j	reaction j
K	key component
l	permeate side
M	methanol
CO	carbon monoxide
*	dimensionless
opt	optimal
W	water

Although many high temperature resistant polymers such as PTFE, PDMS and PPESK (poly (phthalazine ether sulfone ketone)) etc. [9–11] have been synthesized, most membranes formed by these materials need support, due to the thickness and low permeation rate of self-supported membrane. Polymeric support materials also encounter the similar limitation. Inorganic materials have many good physical and chemical properties, especially in the high temperature and corrosive circumstance, but poor separation performance due to the limitation of Knudsen diffusion. Novel composite membranes combining polymer with ceramic, which has high performance and high-temperature resistance as well, is a new research topic to which much attention has been paid recently. Now, silicon rubber/ceramic composite membranes, successfully developed in the authors' laboratory [12,13], combining the high selectivity and high permeation flux of silicone rubber (SR) towards water and organic vapor such as methanol, as well as the excellent mechanical, thermal and chemical stability and negligible mass transfer resistance of ceramic membrane, are expected to have excellent separation property and permeability and have potential applications in the membrane reaction process of methanol synthesis from CO_2.

To formulate the membrane reactor model is the fundamental task for the simulation of the process behaviors of a membrane reactor. Tsotsis et al. [14] set up a relatively general model, the packed bed catalytic membrane reactor model (PBCMR). In that model, the membrane tube having catalytic activities separates the tubular reactor into tube side and shell side, both sides of the membrane packed with catalysts. Many tubular membrane reactors are special cases by simplifica-

tion of this model. For example, the inert membrane packed bed reactor used in this article is a case with the catalyst packed in the shell side, while no catalyst inside the membrane and in tube side.

However, Tsotsis et al.'s model does not consider the effect of the non-uniform distribution of membrane permeation rate. Since the maximum reactant concentration is at the inlet of the membrane reactor, consequently, more loss is there due to the reactant permeation. Mohan and Govind [15] brought out the issue that to decrease the reactant permeation is one of the effective methods to improve conversion. Ye [16] discussed this problem theoretically, pointing out that the conversion by applying a membrane with non-uniform distribution permeation rate along the catalytic bed direction exceeds that with a uniform distribution membrane. Non-uniform distribution of membrane permeation rate means the membrane permeation flux at the membrane reactor inlet is 0, while the remaining part is applied with a uniform and proper membrane permeation rate.

In 1997, the Kyoto protocol was signed, which puts limits to the emission of CO_2. Thus, how to utilize CO_2 with rationality has become a challenge to face in the 21st century. To synthesize methanol from CO_2 is an effective path that is well worthy of thoroughly studying. It is therefore taken as a model reaction in this article. The objective of this study is to theoretically analyze the behaviors of the membrane reactor in a systematical manner based on a one-dimensional isothermal pseudo-homogeneous parallel flow model with non-uniform distribution of membrane permeation rate incorporated [17]. Some theoretical results were verified by experimental results as seen subsequently.

2. Experimental

2.1. Preparation of composite membrane

Solution of SR was prepared from Sylgard-184 precondensate and its curing agent (ratio of curing agent to precondensate is 1:10 in weight) with 120# gasoline as solvent. The substrate of α-Al_2O_3 ceramic tube was purchased from Dalian Institute of Chemical Physics, Chinese Academy of Sciences.

Polymerization–pyrolysis method was adopted to modify the substrate [18,19] as follows: substrate was first dip-coated into SR solution with weight concentration of 5–20%, and then dried at room temperature for 24–72 h. The coated substrate was slowly heated to 300–350 °C and kept the temperature for 3 h. Afterwards, the temperature was increased and stayed at 400–500 °C for 3–5 h in order to remove the organic compound completely.

The substrate modified was dip-coated with SR solution of 0.5–10% and cured to form membrane at room temperature for 72 h. The performance of silicone rubber/ceramic composite membrane was characterized by measuring gas (such as O_2, N_2) permeability in the permeation test unit. It was regarded as defect-free composite membrane when selectivity of oxygen to nitrogen of the composite membrane reaches 90% of that of pure polymer, 2.0 at room temperature.

2.2. Experimental facility and analytical method

Fig. 1 shows the experimental flowsheet and Fig. 2 shows the schematic diagram of membrane reactor. The designed membrane reactor with a stainless steel shell (Φ28 × 2 mm) is 200 millimeter (mm) long and the silicone rubber/ceramic membrane pipe has an outer diameter of 14 mm, while the length of the permeating membrane, l_1, is 150 and 50 mm, respectively.
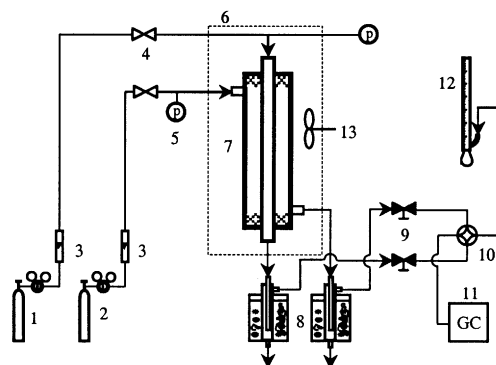
Fig. 1. Flow diagram of membrane reaction system: 1, purge gas cylinder; 2, feed cylinder; 3, gas rotary flowmeter; 4, cut-off valve; 5, pressure gauge; 6, oven; 7, membrane reactor; 8, cold trap; 9, regulating valve; 10, four-way valve; 11, gas chromatograph; 12, soap bubble flowmeter; 13, electric fan.
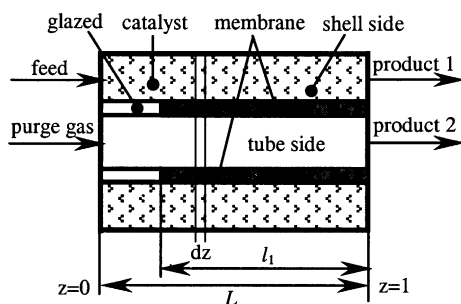
Fig. 2. Schematic diagram of membrane reactor.

Table 1
Relative selectivity to H_2 under different temperature

T (°C)	CO/H_2	CO_2/H_2	CH_4/H_2	Ar/H_2	$MeOH/H_2$	H_2O/H_2
200	0.30	0.558	0.466	0.261	1.125	3.036
210	0.296	0.529	0.455	0.258	1.056	2.876
220	0.292	0.502	0.445	0.256	0.924	2.756
230	0.287	0.479	0.436	0.254	0.868	2.468

The permeation rate of hydrogen through the membrane can be denoted as $J_{H_2} = 3.126 \times 10^{-4} e^{-6600/RT}$ m^3/m^2 s MPa. The relative selectivities of other components to hydrogen are listed in Table 1.

The reaction was carried out in the shell side. The amount of C301 catalyst (Cu–Zn–Al) packed was 6.24 g, with the same size as those used in the reaction kinetic experiment, viz. 0.45 mm, and the catalyst was diluted with quartz of the same size. In the tube side, inert gas Ar was used as sweeping gas. The membrane reactor was placed in a thermostat and the feed enters the shell side via pre-heating coil. Water and methanol were removed from the exit gas of both sides by cold trap, while the dry gas entering GC and soap bubble flowmeter for analyzing the composition and measuring the flow rate, respectively.

The reaction pressure was 0.3–1.6 Mpa, temperature was 200–230 °C. The feeding gas had a mole composition of 66.224% H_2, 25.552% CO_2 and 8.224% CH_4 given by GC.

In the experiment of analyzing the effect of non-uniform distribution parameter L_1 of membrane permeation rate, the permeation length l_1 of membrane used was 50 mm. By changing the filling mode of the catalyst in the shell side, the length L of the catalyst bed can be adjusted to 50, 67, 100, 150 or 200 mm, so that L_1 is 1.0, 0.75, 0.5, 0.33 and 0.25, respectively. Keeping the total amount fixed, the catalyst is uniformly packed in the shell side of the reactor, homogeneously diluted with quartz, Fig. 2. In other experiments, the permeation length l_1 of membrane used was 150 mm and the catalyst bed length L was 200 mm, to give a L_1 of 0.75.

3. Mathematical model

Several assumptions were made as follows:

1) One dimensional plug flow in both shell and tube sides;
2) The reactor is operated isothermally;
3) The membrane tube diameter is far smaller than the tube length and much larger than the particle diameter, neglecting the axial mass and energy diffusion;
4) The gas is ideal;
5) The axial pressure drop on both sides of membrane is negligible;
6) The radial concentration and temperature gradient between gas stream zone and catalyst, and inside the catalyst pellet as well are also negligible.

Thus: shell side

$$\frac{dF_i}{dl} = \rho S \sum_{j=1}^{m1} \upsilon_{i,j} r_j - \beta(l) N_i / l_1, \qquad (1)$$

tube side

$$\frac{dQ_i}{dl} = \beta(l) N_i / l_1, \qquad (2)$$

where

$$\beta(l) = \begin{cases} 0(l_1) & l_1 = 0 \\ 0, & 0 \leq l < L - l_1, \ l_1 \neq 0 \ ; \quad 0 < l \leq L \\ 1, & L - l_1 \leq l \leq L, \ l_1 \neq 0 \end{cases} \qquad (3)$$

Initial conditions: $l = 0$; $F_i = F_{i,0}$; $Q_i = Q_{i,0}$.

Reaction rate

$$r_j = k_{j,+} f_j \left(\breve{p} \right). \qquad (4)$$

Permeation rate of component i

$$N_i = \frac{P_i}{l_m} (p_{h,i} - p_{l,i}) A_m. \qquad (5)$$

And let

$$J_i = \frac{P_i}{l_m} \quad (i = 1, 2, \ldots, n).$$ (6)

Taking H_2 as key component (using subscript k for it), we define the membrane separation factor:

$$\alpha_i = \frac{P_i}{P_k}.$$ (7)

Define dimensionless parameters,

$$z = \frac{l}{L}, \quad L_1 = \frac{l_1}{L}, \quad x_i = \frac{F_i}{F} = \frac{P_{h,i}}{p_h},$$

$$y_i = \frac{Q_i}{Q} = \frac{p_{l,i}}{p_l}, \quad F_i^* = \frac{F_i}{F_0}, \quad Q_i^* = \frac{Q_i}{F_0}, \quad p_r = \frac{p_l}{p_h},$$

$$q_1 = \frac{Q_0}{F_0}, \quad Da = \frac{\rho V_{cat} k_{1,+}}{F_0}, \quad f_j = \frac{r_j}{k_{1,0}},$$

$$\Phi = \frac{1}{L_1} \frac{A_m P_k p_h}{l_m \rho V_{cat} k_{1,0}}, \quad K_j = \frac{k_{j,+}}{k_{1,+}}.$$

So dimensionless formula is drawn as follows:
Shell side

$$\frac{1}{Da} \frac{dF_i^*}{dz} = \sum_{j=1}^{m1} \upsilon_{i,j} K_j f_j(\tilde{x})$$
$$- \beta(z)\alpha_i \Phi(x_i - p_r y_i).$$ (8)

Tube side

$$\frac{1}{Da} \frac{dQ_i^*}{dz} = \beta(z)\alpha_i \Phi(x_i - p_r y_i),$$ (9)

where

$$\beta(z) = \begin{cases} 0\,(L_1) & (L_1 = 0) \\ 0 & (0 \leq z < 1 - L_1,\ L_1 \neq 0)\,; \quad 0 < z \leq 1. \\ 1 & (1 - L_1 \leq z \leq 1,\ L_1 \neq 0) \end{cases}$$ (10)

L_1 equals to zero means the membrane is not permeable converging to a fixed bed reactor. L_1 equals to

one means that the membrane has a uniform permeability across the space of the whole catalyst bed. In this equation: 1 was the catalyst activity in the reaction zone; z was the dimensionless axis position; and l_1 was the membrane length with permeability. The concrete position was indicated in Fig. 2.

Initial conditions,

$$z = 0, \quad F_i^* = x_{i,0}, \quad Q_i^* = q_1 y_{i,0},$$

in which, i represents H_2, CO_2, CH_4, CO, CH_3OH, H_2O and Ar. CH_4 is an inert component as internal standard substance.

There are two reactions in the system,
main reaction

$$CO_2 + 3H_2 \Leftrightarrow CH_3OH + H_2O \quad -49.43 \ \text{kJ/mol}$$ (11)

side reaction

$$CO_2 + H_2 \Leftrightarrow CO + H_2O \quad +41.19 \ \text{kJ/mol}$$ (12)
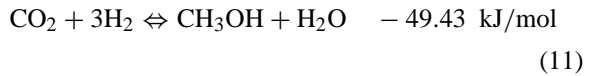
The main reaction is exothermic, and the side reaction is endothermic. The catalytic bed can be kept at a constant temperature state without much difficulty. The hyperbolic type reaction kinetic model obtained experimentally [17] is adopted:

$$f_M(\tilde{x}_i) = \frac{K_{CO_2} K_{H_2}^3 [x_{CO_2} x_{H_2}^3 - x_M x_{H_2O}/(p_h^2 K_{p,M})]}{(1/p_h + K_{H_2} x_{H_2} + K_{CO_2} x_{CO_2} + K_{CO} x_{CO} + K_M x_M + K_{H_2O} x_{H_2O})^4},$$ (13)

$$f_{CO}(\tilde{x}_i) = \frac{K_{CO_2} K_{H_2} (x_{CO_2} x_{H_2} - x_{CO} x_{H_2O}/K_{p,CO})}{(1/p_h + K_{H_2} x_{H_2} + K_{CO_2} x_{CO_2} + K_{CO} x_{CO} + K_M x_M + K_{H_2O} x_{H_2O})^2}.$$ (14)

Based on CO_2, the main reaction conversion X_M to methanol and the side reaction conversion X_{CO} to CO were defined as follow,

$$X_M = \frac{F_M^* + Q_M^*}{x_{CO_2,0}},$$ (15)

$$X_{CO} = \frac{F_{CO}^* + Q_{CO}^*}{x_{CO_2,0}}.$$ (16)

The fourth-order Runge–Kutta method was employed to simulate the process behaviors of the membrane reactor.

4. Results and discussion

4.1. Influence of Da

From the definition, $Da = \rho V_{cat} k_{1,+}/F_0$, Da is the ratio of reaction rate to the feeding rate. For a certain reaction system, when the reaction kinetics was fixed, i.e. $k_{1,+}$ fixed, Da can be regarded as dimensionless residence time. Besides the influence of Da on reaction similar to that of conventional process, viz. reaction conversion increases when Da increases, in the membrane reaction process, the extent of Da's influence was also dependent on membrane permeation parameter Φ. When Φ is large, Da's influence is more notable as seen in Fig. 3.
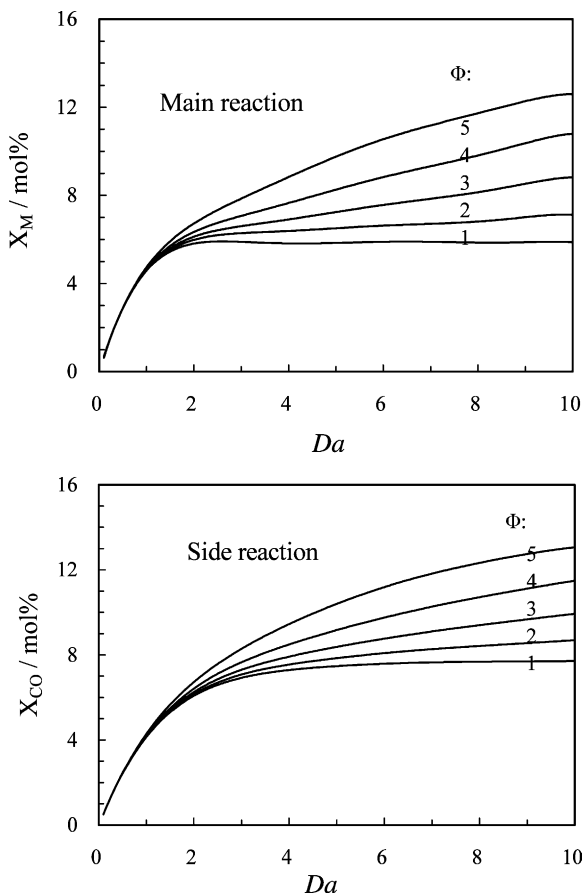
Fig. 3. Conversion versus Da at $T = 200\,^{\circ}\text{C}$, $p_r = 0.1$; $\alpha_M = 2$; $\alpha_W = 6$; $q_1 = 1$; $\chi_{CH_4} = 0.1$; $\gamma = 3$, $L_1 = 1$. Simulation curve: 1, $\Phi = 0$ (f); 2, $\Phi = 0.01$; 3, $\Phi = 0.025$; 4, $\Phi = 0.05$; 5, $\Phi = 0.10$.
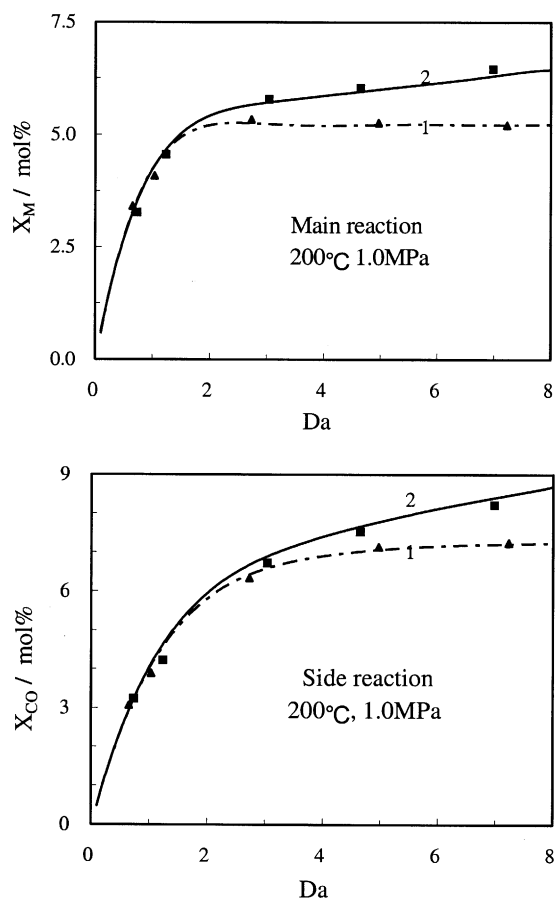
Fig. 4. Effect of Da: ■, experimental data in membrane reactor; ▲, experiment data in fixed bed reactor. Simulation curve: 1, f; 2, $\alpha_M = 1.0$, $\alpha_W = 3.0$.

Fig. 4 illustrated the effect of Da on reaction process at the condition of 200 °C and 1.0 MPa. By changing the flow rate of feed gas, Da can be adjusted at different values. The maximum Da was 7.5 in the experiments due to the restriction of membrane permeation flux. The experimental results showed that the conversions of both main and side reactions increased when Da increased. However, when Da was small, the potential function of membrane reactor was not fully displayed because reaction was kinetically controlled. Only when there was a relative long contact time, which means, reaction approaches its equilibrium status, can the membrane break through the limitation of equilibrium. It was

shown that Da equals to about 7.0, the conversions of main reaction in fixed bed reactor and membrane reactor were 5.23 and 6.4%, respectively, showing about 22% higher in the latter than in the former reactor.

4.2. Membrane separation factor

The main and side reactions had the same product H_2O. Thus, the membrane separation factors of methanol, water and CO to H_2 (denoted as α_M, α_W and α_{CO}, respectively) determine the conversion of the main and side reactions. α_{CO} was as low as around 0.30 in the range of reaction temperature, while α_M, α_W varied with temperature. At low tem-

peratures, the selectivity was high; when temperature increased, the separation factor dropped. As shown in Fig. 5, when Φ was fixed, the main reaction conversion X_M increased with the increase of α_M and α_M. When α_M rose from 0.5 to 2.0, the conversion also increased. When α_W was kept constant, the main reaction conversion increased with the increase of α_M, while the side reaction conversion decreased; when α_M increased to a certain value, the side reaction conversion began to below its equilibrium conversion (sign '1' is the result of fixed bed reactor in nether Fig. 5). From the reaction engineering point of view, it was clear that when α_M rose, the main reaction rate increased, consequently, inhibiting the process of side reaction. It was more prominent
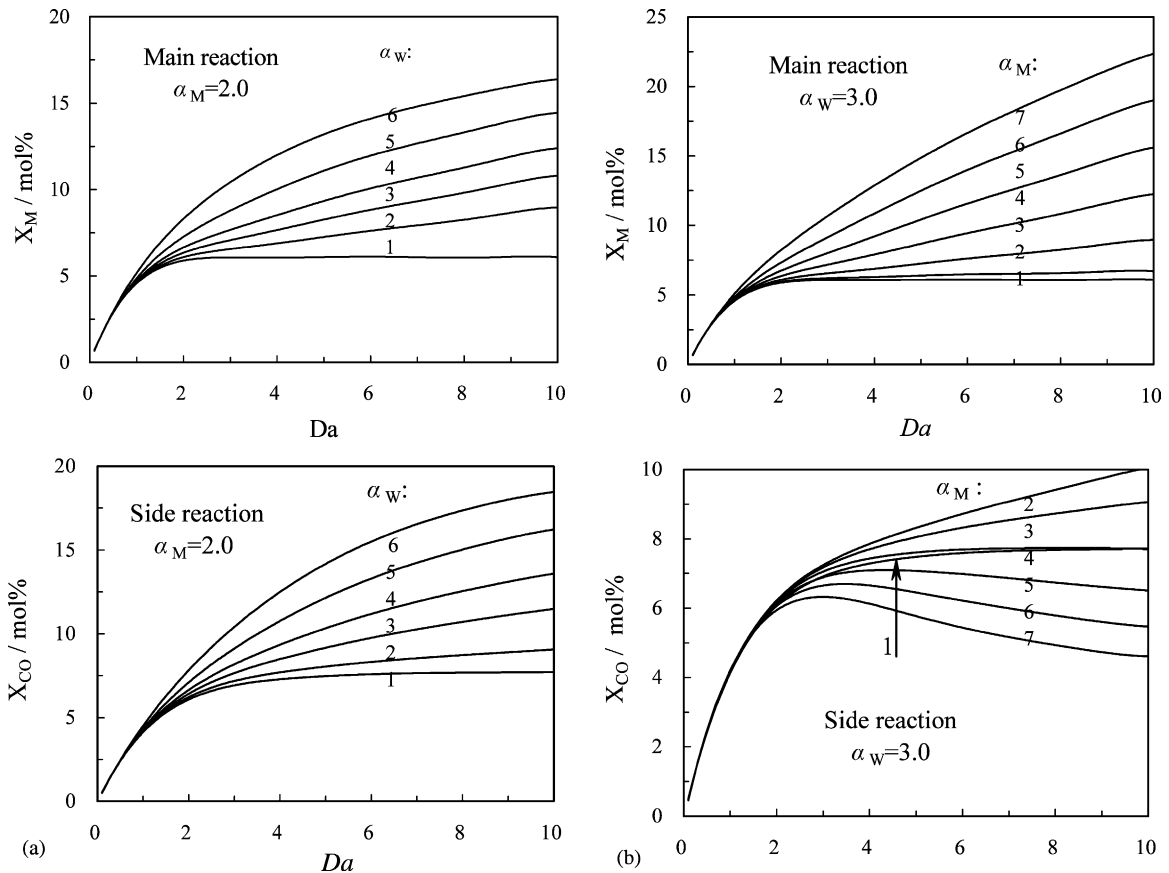
Fig. 5. Conversion versus a with $T = 200\,°C$, $p_r = 0.1$; $\Phi = 0.05$; $q_1 = 1$; $\chi_{CH_4} = 0.1$; $\gamma = 3$, $L_1 = 1$. (a) $\alpha_M = 2.0$; α_W: 1, f; 2, 3.0; 3, 6.0; 4, 10.0; 5, 20.0; 6, 50.0. (b) $\alpha_W = 3.0$; α_M: 1, f; 2, 0.5; 3, 2.0; 4, 5.0; 5, 10.0; 6, 20.0; 7, 50.0.

for the case of small water membrane separation factor.

4.3. Membrane permeation rate

Fig. 6 showed that, when the membrane separation factor was fixed, there exists an optimal membrane permeation rate parameter Φ, respectively for the main and side reactions. The optimal membrane permeation parameter Φ_{opt} varies with Da and the membrane separation factor. When Da was fixed and the membrane permeation rate exceeded the optimal value, the reactant permeation also increased, which diminished the opportunities of the reactant passing through the catalyst bed and lead to the decrease of the overall selectivity.
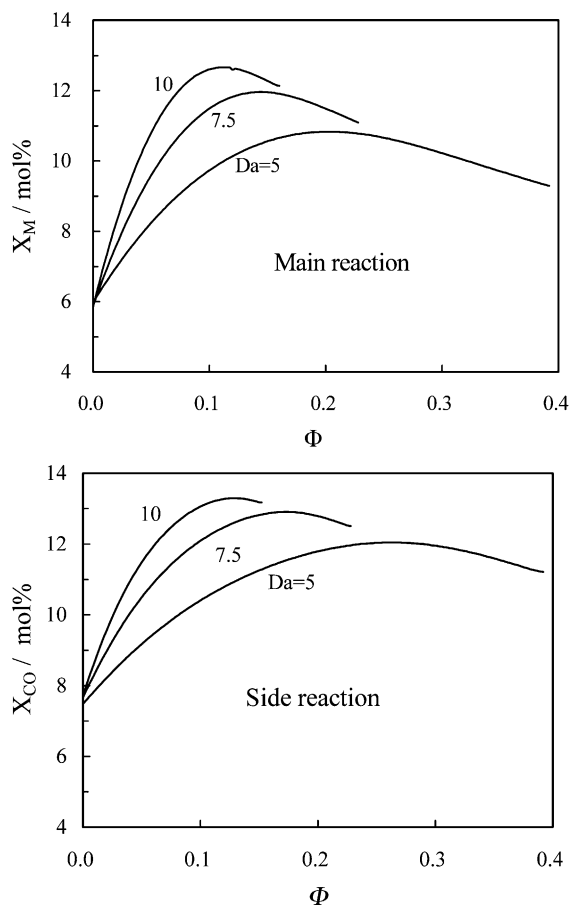
Fig. 6. Conversion versus permeation rate $T = 200\,^{\circ}\mathrm{C}$, $p_r = 0.1$; $\alpha_M = 2$; $\alpha_W = 6$; $q_1 = 1$; $\gamma = 3$, $L_1 = 1$.

4.4. Pressure ratio p_r

The pressure ratio p_r influences the main and side reaction conversion as what Fig. 7 indicated. The membrane permeate side was kept at atmospheric pressure, so the pressure ratio p_r was determined by reaction pressure p_h. By increasing p_h, the permeation rate of the component with large membrane separation factor will increase consequently. Thus, when the main and side reactions were reversible, both of their conversions exceeded their equilibrium conversions especially at large Da. Since the reaction is a complex parallel system, with the increase of the pressure, the conversion of the main reaction increases. On the contrary, the conversion of the side reaction had a maximum value at a given p_h. At a low pressure, the side reaction was controlled by kinetics and its conversion was below the thermodynamic equilibrium conversion. As the pressure gradually rose, the reaction process became limited by the thermodynamic equilibrium and at this time the conversion of the side reaction transits from close to the equilibrium conversion to exceeding the equilibrium conversion until it arrived at the maximum conversion. Further increase of pressure resulted in the increase in the rate and the conversion of the main reaction so as to inhibit the progress of the side reaction. Thus the side reaction conversion decreased. To increase the pressure was advantageous to the main reaction; therefore, within the acceptable pressure limit of the membrane, as high a reaction pressure as possible should be applied.

4.5. Reaction temperature T

The effect of temperature on the reaction was complex. The temperature variation will cause the changes of thermodynamic equilibrium of the reaction, membrane separation performance and catalyst activity. Since, the activation energies of the main and side reaction are 90.52 and 138.41 kJ/mol, respectively [17], the reaction rates increased 1.5 and 2.0 times with 10 °C temperature increase, respectively. The permeation activation energy of H_2 is 6.6 kJ/mol, and within the range of the reaction temperature used in the experiments the increase of its permeation rate was not obvious. The permeation rate of those condensable products like
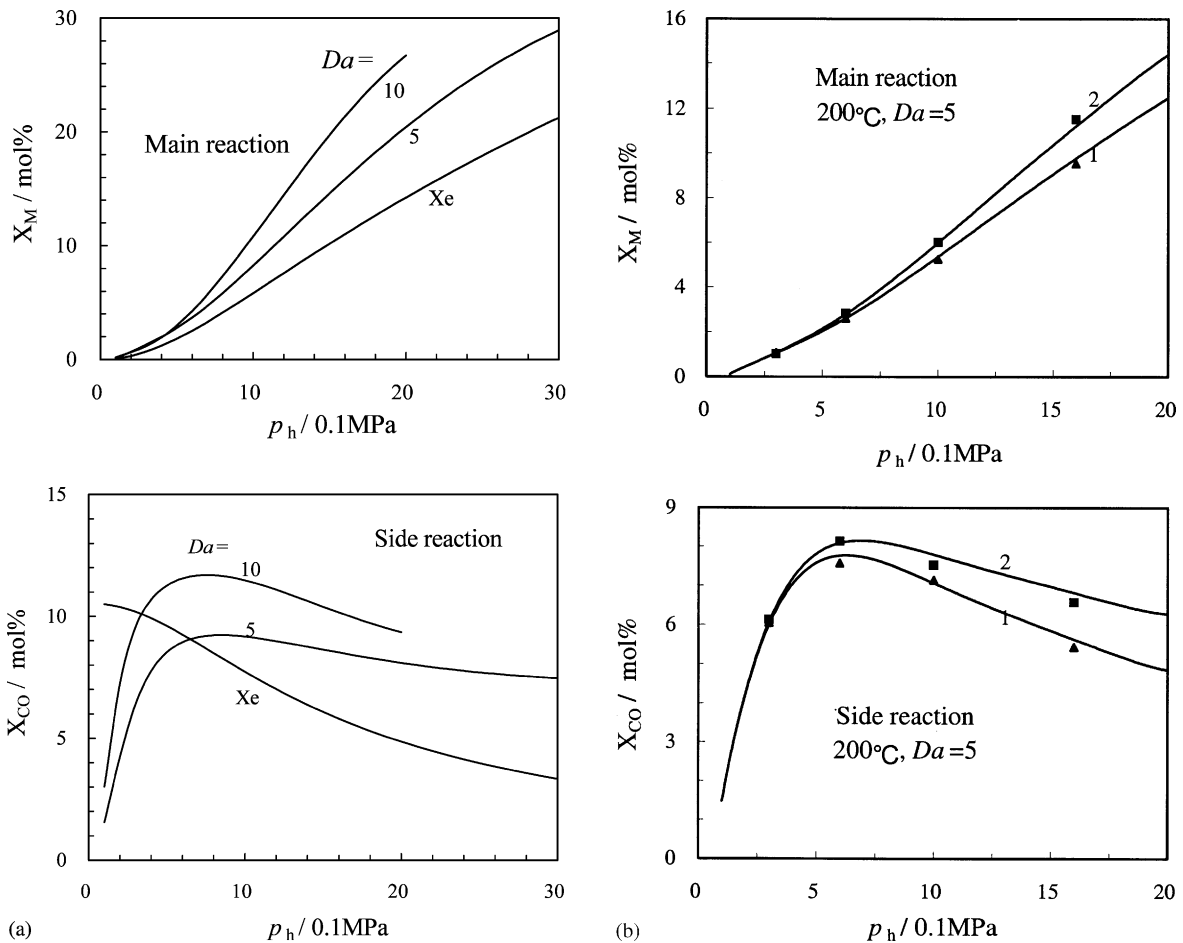
Fig. 7. Effect of reaction pressure. (a) Simulation results at $T = 200\,°C$, $\Phi = 0.05$; $\alpha_M = 2$; $\alpha_W = 6$; $q_1 = 1$; $\chi_{CH4} = 0.1$; $\gamma = 3$, $L_1 = 1$. (b) ■, experimental data in membrane reactor; ▲, experiment data in fixed bed reactor. Simulation curve: 1, fixed bed reactor; 2, membrane reactor, $\alpha_M = 1.0$, $\alpha_W = 3.0$.

methanol and water will however decrease with the increase of temperature. Hence, the membrane separation factor was lowered. The silicone rubber/ceramic composite membrane in the experiment will lower its methanol separation factor from higher than 1.0 to less than 1.0 when the reaction temperature exceeded 215 °C. It can be observed from Fig. 8 that low temperature favors the main reaction. At high temperatures, the side reaction rate increased faster and methanol membrane separation factor decreased, causing the main reaction conversion to approach that in the fixed bed reactors. The conversion of the side reaction was

larger than its equilibrium conversion of 10.1% at 218 °C.

4.6. Effects of L_1

To diminish the feed loss through reactant permeation in the membrane reactor, non-uniform distribution of membrane permeation rate L_1 was applied as described by Eq. (10). In order to testify the effects of this non-uniform distribution on the membrane reactor behaviors, the effective membrane length adopted in the experiment occupied one-fourth of the total reaction zone height, i.e. l_1 is 50 mm.

Through varying the catalyst bed height L at 50, 67, 100, 150 and 200 mm, respectively, L_1 was adjusted to different values such as 1.0, 0.75, 0.5, 0.33 and 0.25.

Simulation results are shown in Fig. 9, where line '1' ($L_1 = 0$) means fixed bed reactor, and line '3' ($L_1 = 1$) represents the membrane reactor with uniform distribution. When $L_1 = 0.1$, the conversion in membrane reactor was lower than that with the uni-

form distribution. Only when L_1 increased to 0.4, can the conversion of the membrane reactor with non-uniform distribution exceed that with uniform distribution. The effect of L_1 can be better seen in Fig. 10 where the conversions are plotted against L_1 at a given Da of 5. The main and side reactions conversions are all higher than the values for fixed bed reactor. The L_1 value shows the maximum effect when it is between 0.50 and 0.75 where conversions for main and side reactions reach 6.26 and 7.96%, higher than their corresponding equilibrium conversions of 5.24 and 7.28%, respectively.
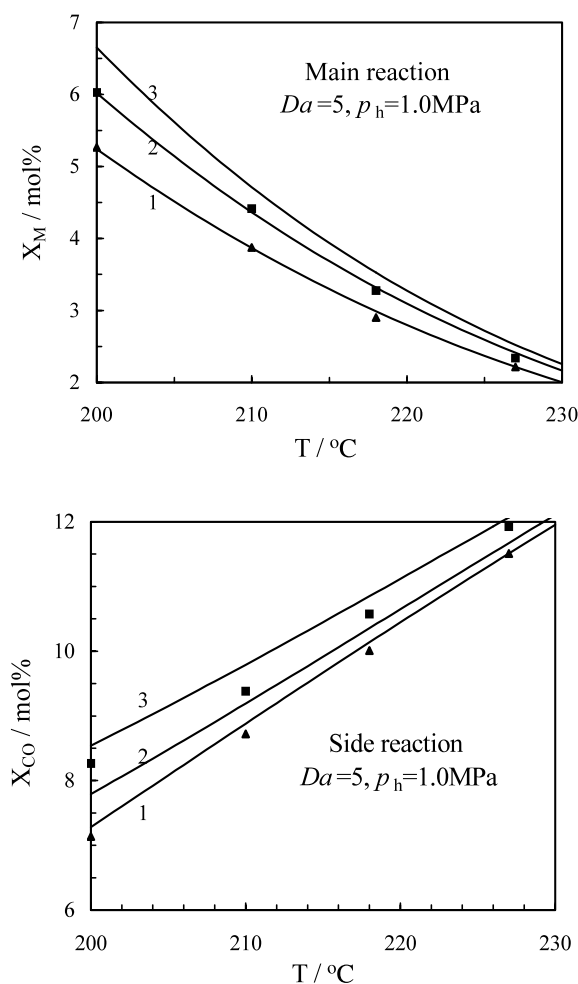
Fig. 8. Effect of reaction temperature: ■, experimental data in membrane reactor; ▲, experiment data in fixed bed reactor. Simulation curve: 1, fixed bed reactor; 2, membrane reactor, $\alpha_M = 1.0$, $\alpha_W = 3.0$; 3, membrane reactor, $\alpha_M = 1.0$, $\alpha_W = 5.0$.
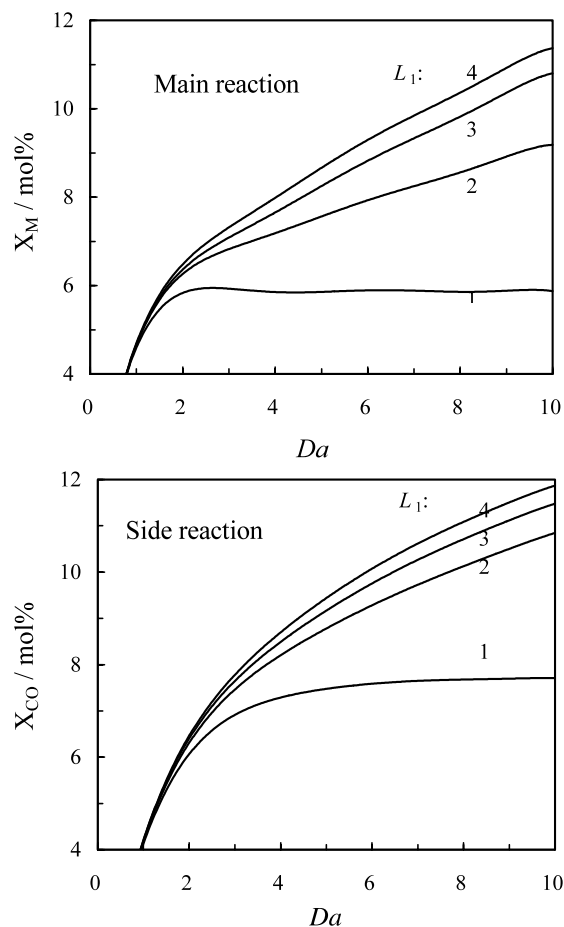
Fig. 9. Conversion versus Da $T = 200\,^\circ$C, $\Phi = 0.05$; $p_r = 0.1$; $\alpha_M = 2$; $\alpha_W = 6$; $q_1 = 1$; $\chi_{CH_4} = 0.1$; $\gamma = 3$, $q_1 = 1$. Simulation curve: 1, $L_1 = 0$; 2, $L_1 = 0.1$; 3, $L_1 = 1.0$; 4, $L_1 = 0.8$.
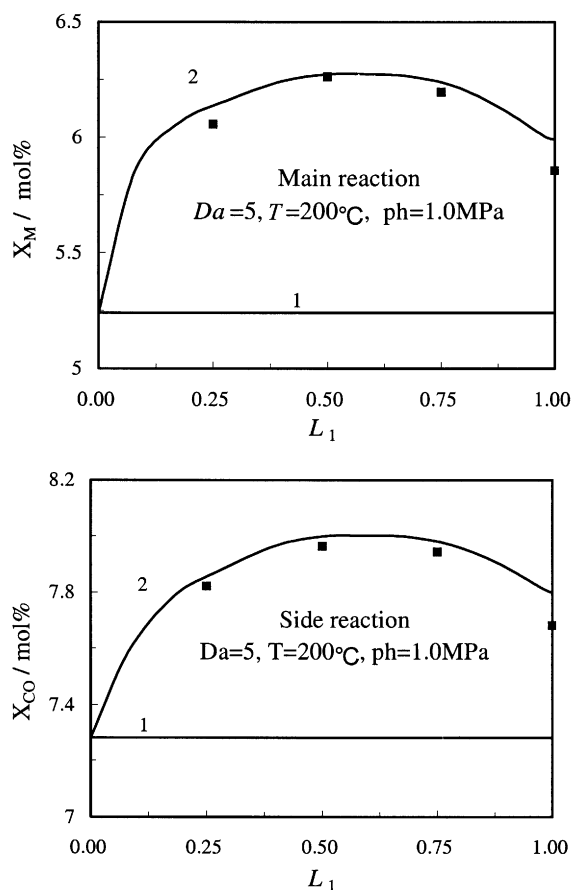
Fig. 10. Effect of L_1 on reaction behavior: ■, experimental data in membrane reactor. Simulation curve: 1, fixed bed reactor; 2, membrane reactor, $\alpha_M = 1.0$, $\alpha_W = 3.0$.

5. Conclusion

The influence of Damköhler number on the reaction behavior in the membrane reactor was similar to that in the fixed bed reactor, but the extent depends on the membrane permeation parameter Φ and membrane separation factor α. The latter had more influences. Viewed from the reaction engineering point of view, when the methanol selectivity increased, the main reaction speeded up and the side reaction was inhibited, resulting in an increase in main reaction conversion. There was an optimal membrane permeability parameter Φ_{opt}, giving a maximum main reaction conversion. Parts of theoretical analysis results had been exam-

ined by experimental results. Under the experimental conditions studied, the main reaction conversion increased from 5.23 to 6.4%, i.e. 22% higher than that in the traditional fixed bed reactor. The theoretical analysis and experimental results showed that non-uniform excelled uniform in the distribution of membrane permeation rate when L_1 was in a certain range, and there exists an optimal L_1 value for the reaction process.

References

[1] A.S. Michaels, Chemical Engineering Progress 64 (12) (1968) 31.

[2] T.M. Raybold, M.C. Huff, Studies in Surface Science and Catalysis 110 (1997) 501.

[3] Y. She, J. Han, Y.H. Ma, Catalysis Today 67 (2001) 43.

[4] G. Barbieri, F.P. DiMaio, Industrial and Engineering Chemistry Research 36 (1997) 2121.

[5] R. Zhao, R. Govind, N. Itoh, Separation Science and Technology 25 (1990) 1473.

[6] F.T. Akin, Y.S. Lin, Journal of Membrane Science 209 (2002) 457.

[7] H.H. Wang, Y. Cong, W.S. Yang, Journal of Membrane Science 209 (2002) 143.

[8] R.P.W. Struis, S. Stucki, M. Wiedorn, Journal of Membrane Science 113 (1996) 93.

[9] R. Holze, J.C. Ahn, Journal of Membrane Science 73 (1992) 87–97.

[10] P. Sampranpiboon, R. Jiraratananon, D. Uttapap, X. Feng, R.Y.M. Huang, Journal of Membrane Science 174 (2000) 55–65.

[11] X.G. Jian, Y. Dai, G.H. He, G.H. Chen, Journal of Membrane Science 161 (1999) 185–191.

[12] G.W. Chen, Q. Yuan, Journal of Chemical Engineering of Chinese University 15 (2001) 420–424.

[13] G.W. Chen, Q. Yuan, D.Y. Wu, G.Z. Fu, Journal of Chemical Industry and Engineering (China) 51 (2000) 725–731.

[14] T.T. Tsotsis, R.G. Minet, A.M. Champagnie, P.K.T. Liu, in: E.R. Becker, C.J Pereira (Eds.), Computer Aided Design of Catalysts, Vol. 51, Marcel Dekker, Chemical Industry, New York, NY, 1993, p. 471 (Chapter 12).

[15] K. Mohan, R. Govind, AIChE Journal 34 (1988) 1493.

[16] J.B. Ye, Gas Phase Catalytic Reaction on Membrane Reactor: [dissertation], Dalian, Institute of Chemical Physics, Chinese Academy of Sciences, 1990

[17] G.W. Chen, Q. Yuan, Journal of Chemical Industry and Engineering (China) 53 (2002) 17–22.

[18] D. Li, S.T. Hwang, Journal of Membrane Science 59 (1991) 331–352.

[19] C.W. Jone, W.K. Koros, Industrial and Engineering Chemistry Research 34 (1995) 158–163.